TU/e and IPP Greifswald

Internship

First steps towards designing and modeling plasma heating for a future Stellarator type reactor

Tim Heiszwolf (1242343)

November 29, 2024

Abstract

Any future fusion (Stellarator) reactor is going to require plasma heating. In this report options for Electron Cyclotron Resonance Heating (ECRH) are investigated and proof of concept ECRH beams are designed for various (future) reactors. To accomplish this a novel ECRH region-plot was made to quickly investigate possibilities and the ray tracing code Travis was used to 'empirically' determine feasibility. The model showed good results for a slow-X-mode beam launched from the lower inboard side of ITER. And for a potential magnetic configuration for a future Stellarator, SQuID, it was found that in the turning points of the reactor a saddle-point could be found and exploited for slow-X-mode from the inboard, outboard and upper and lower parts of the inboard-side. Also a more conventional O-mode was found to be possible in a section of the reactor with a significantly lower magnetic field.

Contents

1 Introduction

With the ever increasing power consumption of humanity fusion power could, in the future, play a crucial role in satisfying such demand. However commercial fusion reactors still have many decades of development left. Undoubtedly development or large reactors with higher density/magnetic field will be required. Thus one of the challenges is how to heat the plasma is such larger reactors. Electron Cyclotron Resonance Heating (ECRH) is a method that is often considered for such future reactors. In this internship report various ECRH method will be discussed and used to design beams for reactors. It was made at the Max Planck Institute for Plasma Physics in Greifswald, Germany where extensive research into ECRH is being done and where they also currently have the largest Stellarator device in the world.

First the theory behind ECRH, the various method and engineering limitations will be discussed. Here a focus will be on a unique region-plot which can be used to clearly see ECRH transmission, cutoff, resonance and through which the path of ECRH beams can be plotted and thus can be used to quickly estimate the results of those beams.

Next the ray tracing code Travis is used to "empirically" (re)design beams. To do this several challenges related to file conversion and compatibility with Travis had to be overcome. This was done for several fusion devices. First as a interesting exercise new ECRH beams for Wendelstein-7X were investigated/designed. Next this was also done for the ITER Tokamak. While it is not a Stellarator it is one of the large future fusion reactors which also is going to need heating. While certain issues related to permission and file conversion/compatibility were being solved a hypothetical high-field version of Wendelstein-7X was also redesigned. Finally, once the issues had been sorted out, ECRH beams for the SQuID magnetic configuration were designed/investigated. SQuID is a recently developed magnetic configuration which could potentially be used in future Stellarator reactor [5].

2 Theory and background

2.1 Electron Cyclotron Resonance Heating

For Electron Cyclotron Resonance Heating (ECRH) the two most important frequencies in a fusion plasma are the electron gyration frequency and the plasma frequency. The plasma frequency is

$$\omega_p = \sqrt{\frac{n_e q_e^2}{\epsilon_0, m_e}} \tag{1}$$

where ω_p is the plasma (angular) frequency, n_e is the electron density, q_e is the electron charge, ϵ_0 is the vacuum permittivity and m_e is the electron mass. The (electron) cyclotron frequency is

$$\omega_{ce} = \frac{q_e B}{m_e} \tag{2}$$

where ω_{ce} is the electron cyclotron frequency, B is the magnetic field strength.

If a electromagnetic beam is send into the plasma at a harmonic of this electron cyclotron frequency resonance can happen which heats the plasma

$$\omega_{absorp} = n\omega_{ce} \tag{3}$$

where n is a integer representing the harmonics [6]. Finally there also is an upper hybrid frequency

$$\omega_{uh} = \sqrt{\omega_p^2 + \omega_{ce}^2} \tag{4}$$

where ω_{uh} is the upper hybrid frequency [6].

However this beam might not always be able to penetrate the plasma, it can be cutoff. This can be determined via the index of reflection (derived from the Appleton-Hartree equation). For O-mode that is

$$N_O = 1 - \frac{\omega_p}{\omega} \tag{5}$$

where N_O is the refraction index, ω is the (angular) frequency of the beam [6] which results in a cutoff at

$$\omega_O = \omega_p \tag{6}$$

where ω_O is the O-mode cutoff frequency.

For X-mode a more complex equation can be found

$$\begin{aligned} \omega_L &= \frac{1}{2}\left(\sqrt{\omega_{ce}^2 + 4\omega_p^2} - \omega_{ce}\right) \\ \omega_R &= \frac{1}{2}\left(\sqrt{\omega_{ce}^2 + 4\omega_p^2} + \omega_{ce}\right) \\ N_X &= \frac{(\omega^2 - \omega_L^2)(\omega^2 - \omega_R^2)}{\omega^2(\omega^2 - \omega_{uh}^2)} \end{aligned} \tag{7}$$

where N_X is the index of refraction, ω_L is the left cutoff frequency which cuts off the so-called slow-X-mode which can transmit until the upper hybrid frequency ω_{uh} and the ω_R is the right cutoff frequency above which transmission is possible again in so called fast-X-mode [6]. This results in a sort of band-structure which can be seen in figure 1a.

There are three variables the equalities for the X-mode cutoff, f, n_e and B all of which can be used to plot the refraction index and cutoffs (see figure 1). From such a plot the cutoff for fast-X-mode, which could be seen as the "normal" X-mode, can be seen. However one can also see the slow-X-mode regions which allows for lower beam frequencies, higher densities and/or magnetic fields. Lower frequencies are desirable due to constraints on gyrotron output and higher densities/magnetic fields are desired for reactor performance. Due to these cutoff bands it

might seem impossible to reach this slow-X-mode. In chapter 2.3.3 methods for using this regime are discussed.

It should be noted that slow and fast-X-mode are the same in terms of physics/electromagnetism, the different names are only to indicated in which plasma-regimes the X-mode is [6].

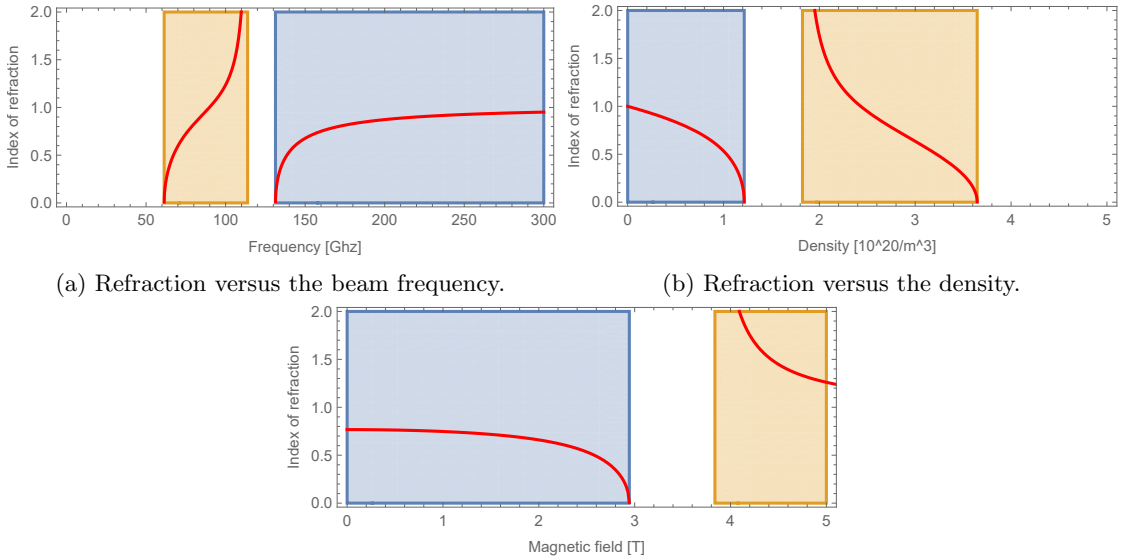

(a) Refraction versus the beam frequency.

(b) Refraction versus the density.

(c) Refraction versus the magnetic field.

Figure 1: Various graphs for the index of refraction of X-mode. Function depends on 3 variables, if not varied kept constant at $f = 140$ GHz, $n_e = 1 \cdot 10^{20}$ m^{-3} and $B = 2.5$ T. The orange represents regions of slow-X-mode transmission and the blue regions fast-X-mode transmission.

These equalities can also be displayed in a region plot which allows one to see how two of the variables effect each other. In figure 2 such a region plot can be seen. The beam frequency f is taken as constant since it remains constant along the beam path. On the x-axis the density is plotted and on the y-axis the magnetic field. For both O and X-mode the regions where the input frequency is sufficient to not be cutoff are colored and bands where this frequency matches a resonances frequency can also be seen.

What makes this plot so useful is the ability to quickly and approximately predict what a beam is going to do (and what can be done to change the behavior). One keeps track or estimates the magnetic field and density along the beam path which can then be traced in the region plot to approximate the beam behavior. If the beam reaches the edge of the transmission region it will likely be cutoff, if a beam goes through a resonance band it will likely be (partially) absorbed, etc. In terms of ECRH design, thus, quickly issues could be seen, and what needs to be changed can be determined by seeing what paths through the region plot are desirable. The beam frequency can also be quickly changed (via a slider in Wolfram Mathematica) to see what effects that would have (a higher beam frequency "pushes" the regions away from the origin while a lower beam frequency "pulls" it towards the origin).

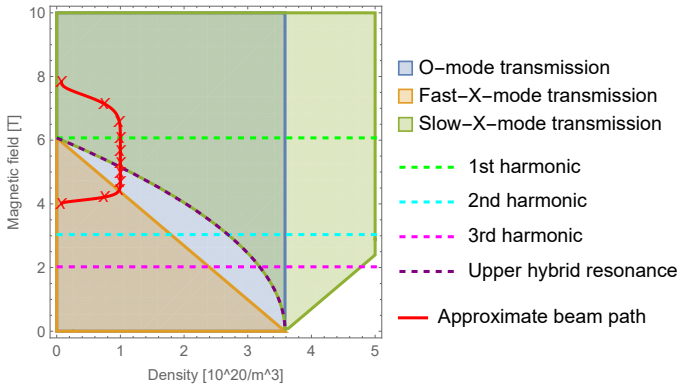

Figure 2: Regions of transmission and resonance for a 170 Ghz beam. The red line is an estimation of the density and magnetic field along a beam through the ITER reactor ($B_0 = 5.3$ T, $n_{e0} = 1 \cdot 10^{20}/\mathrm{m}^3$ [2]), the distance between crosses corresponds to 10% of the beam path length.

2.2 Reactor limitations

Also of interest are the engineering constraints for ECRH. First making high frequency gyrotrons suitable for ECRH is very challenging. ITER is planning to have 170 GHz gyrotrons with a potential future upgrade to 210 GHz gyrotrons [10]. Similarly for CFETR (a future Chinese experimental Tokamak) 230 GHz gyrotrons are being designed [7]. These frequencies will be treated as the upper-limit when designing ECRH beams, however lower frequencies, which can already be reliably used are better.

Another factor is port access. In general making ports on vessels is very difficult and reduces performance; thus as little ports as possible should be used [4]. Further more during the design of the reactors ECRH is often not high on the priority list thus one often has little choice is where and which ports one gets access to. Because of this all kinds of directions should be considered. In figure 3 a overview of the approximate directions can be seen.

Finally is the beam angle. The beam angle can be directly into the plasma, azimuthally or attitudinally (also see figure 3) and often can be steered. ITER has a maximum angle of 45° with up to 25° of steering [10].

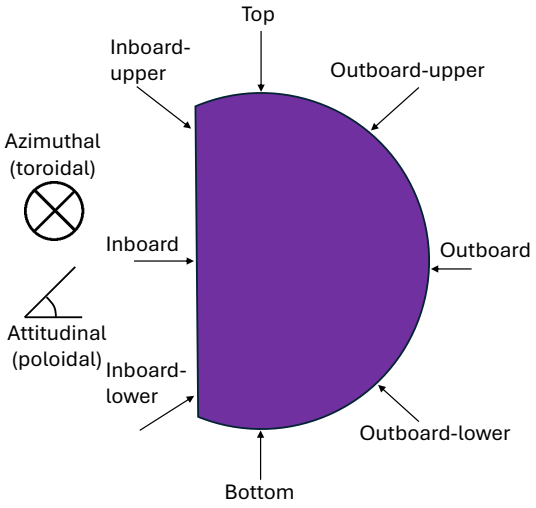

Figure 3: A sketch of a cross-section of a reactor with labels indicating various approximate directions where a port could be located.

2.3 Electron Cyclotron Resonance Heating techniques

2.3.1 O-mode

A very common and basic ECRH technique is O-mode heating. The cutoff is only density depended which makes it relatively easy to design. In general, if the density permits, a lower harmonic is better. Not only due to the lower required frequency of the beam but also since lower harmonics have better absorption [6].

2.3.2 X-mode

Also commonly used is (fast-)X-mode. The frequency used must inherently be higher than the first harmonic since at the first harmonic the cutoff density is 0 (see figure 4). Thus it often is used in the second harmonic. This means that if the magnetic field is to strong then the frequency required is very high. Also the cutoff density is at maximum the same as O-mode while at the second harmonic it is half that. So (fast-)X-mode also is not suitable for high density applications. The advantage of X-mode however is relatively high absorption [6]. This is especially advantageous at lower densities where these lower densities can decrease absorption significantly.

2.3.3 Slow-X-mode

Using slow-X-mode can be a bit tricky due to the cutoff band in the magnetic field and density. Usually ECRH is done from the low-field side which causes the magnetic field to increase along the beam. This causes the wave to start as fast-X-mode and to encounter the cutoff. One could lower the frequency even further to ensure it starts as a slow-X-mode but then it likely will either be immediately absorbed at the edge or won't be absorbed at all. So the solution is to inject the beam from the high-field side.

Similarly to ensure the beam is in slow-X-mode, the beam frequency should be lower than the upper hybrid frequency at zero density. This corresponds to the first electron cyclotron harmonic.. At the same time the picked frequency should be high enough that, as the beam goes from the high-field to the low-field, the cyclotron frequency goes down enough for resonance. Thus the frequency that works best would be (slightly) below (depending on magnetic gradient) the first electron cyclotron harmonic of the target area. In figure 4 it can be seen how this technique could be used for heating where same frequency O-mode and fast-X-mode are unable to.

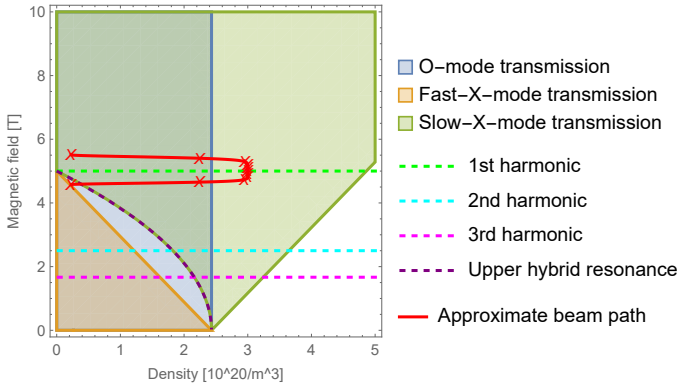

Figure 4: Regions of transmission and resonance for a 140 Ghz beam in a high-field Wendelstein 7X type reactor ($B_0 = 5$ T, $n_{e0} = 3 \cdot 10^{20}/\mathrm{m}^3$).

It also is possible to tunnel through the cutoff band but this can only be done efficiently if the physical size of the cutoff band is approximately the same order of magnitude or smaller as the wavelength (which usually is between 0.1 and 1 centimeter) [3]. That requires a very high

gradient in the magnetic field and/or density which may not be present in all reactors. This method can be used from the low-field side.

2.3.4 Bernstein waves

Another technique for high density plasmas heating is to use Bernstein waves. These waves don't have a density limit but can only exist and be produced inside the plasma [6]. Thus to use Bernstein waves a mode-conversion is required of which two methods will be discussed.

The first method uses O-mode which is converted to (slow-)X-mode and then to Bernstein waves (OXB conversion). O-mode is launched and reaches its cutoff, if this cutoff is located close to the upper-hybrid frequency the wave will be converted from O to slow-X to Bernstein waves [1] (see figure 5). To ensure that the O-cutoff and upper-hybrid resonance are in close proximity to each other it is best to use the second harmonic or higher frequency waves.

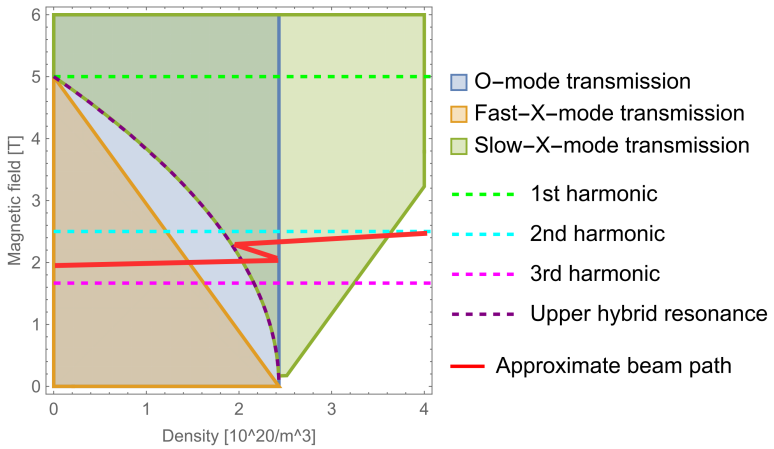

Figure 5: Sketch of 140 Ghz OXB beam in the transmission region plot of a high-field Wendelstein 7X type reactor ($B_0 \approx 5$ T, $n_{e0} \approx 3 \cdot 10^{20}/\mathrm{m}^3$). The reflection after reaching the O-mode cutoff doesn't continue to a higher-field area but goes back the same path, for clarity it is edited such that the lines don't overlap.

The second method converts X-mode directly into Bernstein waves (XB conversion). Either fast-X-mode can be launched, tunnel through the cutoff and then at the upper-hybrid resonance gets converted to Bernstein waves [6] or slow-X-mode can be launched from the high-field side while avoiding the regions of high density (to avoid cutoff but also to avoid premature absorption) until the upper-hybrid resonance is reached where the waves are converted and bounce back into the plasma/to the center [9] (see figure 6).

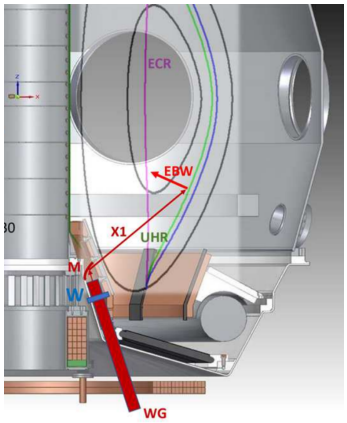

Figure 6: A sketch of XB conversion from the high-field side. Taken from [9].

In the early stages of this report both of these method for using Bernstein waves were attempted but unfortunately no working implementation was found despite considerable effort. Thus for the rest of this report these beams won't be used.

2.3.5 Overview

- O-mode:
  - Less efficient and precise energy transfer. Sometimes requires multiple passes.
  - Easy to design.
  - Reasonable density acceptability. Generally can handle twice the density as same frequency (fast-)X-mode.
  - Cutoff: $n_e \approx 2.4 \cdot 10^{20}$ /m^3 (at $f = 140$ Ghz)
- (Fast-)X-mode
  - Very good and precise energy transfer.
  - Easy to design.
  - Limited density and B-field acceptability.
  - Cutoff: $n_e \approx 1.2 \cdot 10^{20}$ /m^3 (at $f = 140$ Ghz and $B = 2.5$ T) or $n_e \approx 4.9 \cdot 10^{20}$ /m^3 (at $f = 280$ Ghz and $B = 5$ T)
- Slow-X-mode:
  - Less efficient and precise energy transfer.
  - Requires specific conditions and acces points.
  - Great accessibility. Thus requiring a frequency half that of (fast-)X-mode.
  - Cutoff: $n_e \approx 4.9 \cdot 10^{20}$ /m^3 (at $f = 140$ Ghz and $B = 5$ T)
- Bernstein waves:
  - Usually low conversion (and thus heating) efficiency [6].
  - Hard to design.
  - Limitless accessibility.
  - Cutoff: None but has minimum density (OXB must reach O-cutoff, XB must reach upper hybrid resonance).

3 Interesting ECRH configurations

In this chapter several interesting ECRH configurations will be tested, these were all modeled using a ray tracing code called Travis [8]. See appendix A for a tutorial on how to use Travis.

3.1 Wendelstein 7X

A interesting case would be Wendelstein 7X in the current configuration ($B_0 \approx 2.52$ T, $n_{e0} = 0.75 \cdot 10^{20}$ /m^3, $T_{e0} = 5$ KeV).

At the density and magnetic field of the center the first harmonic is at approximately 70 GHz, (fast-)X-mode cutoff is at approximately 120 GHz and the O-mode cutoff is approximately 78 GHz. This means that the first harmonic is not trivial for both modes, but is possible for both at the second harmonic (see figure 7). However slow-X-mode is possible and can even pass through the plasma at frequencies lower than 70 GHz (see figure 7b).

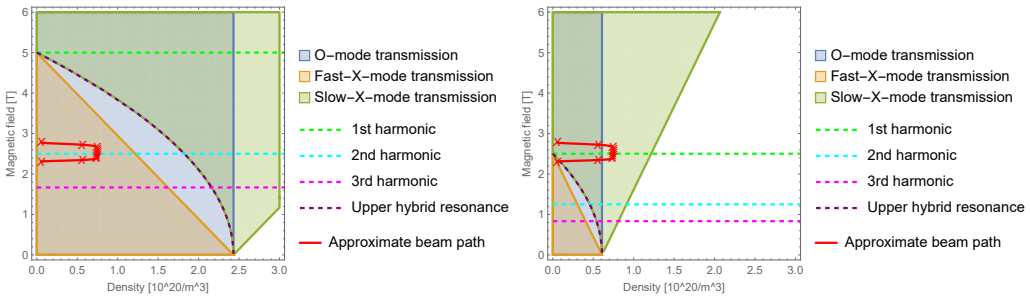

(a) 140 GHz beam.

(b) 70 GHz beam.

Figure 7: Regions of transmission and resonance in Wendelstein 7X ($B_0 \approx 2.52$ T, $n_{e0} = 0.75 \cdot 10^{20}$/m^3).

Table 1: Several beam possibilities for an reactor like W7X. The absorption location is the peak absorption per volume as a fraction of the minor radius and the variation is given in half-width-half-maximum (HWHM). The height of the peak (in case of a 1 MW beam) also is given and can also be seen as a indication of concentration.

Beam location and direction	**Mode and frequency**	**Absorption peak (r/a)**	**Peak (MW/m)/ Absorption**	**Note**
Outboard $\phi = 0$ direct→25 °azimuthal	X 140 GHz	$0.00 \pm 0.02 \rightarrow$ 0.72 ± 0.06	30/100% → 7/100%	
Outboard $\phi = 0$ direct→15 °azimuthal	O 140 GHz	$0.38 \pm 0.27 \rightarrow$ 0.03 ± 0.02	2.1/99% → 6.5/99%	multiple passes
Outboard-upper $\phi = 0$ direct→-30 °attitudinal	X 140 GHz	$0.46 \pm 0.01 \rightarrow$ 0.08 ± 0.05	50/100% → 14/100%	
Outboard-upper $\phi = 0$ direct→-30 °attitudinal→ -30 °attitudinal & 25 °azimuthal	O 140 GHz	$0.48 \pm 0.05 \rightarrow$ $0.10 \pm 0.03 \rightarrow$ 0.00 ± 0.02	6.5/94% → 3.1/98% → 8.0/100%	
Inboard $\phi = 0$ direct→25 °azimuthal	X 66 GHz	$0.06 \pm 0.03 \rightarrow$ 0.85 ± 0.06	1.2/70% → 7.8/97%	wide tails of distribution
Inboard $\phi = 0$ direct→25 °azimuthal	O 117 GHz	$0.04 \pm 0.02 \rightarrow$ 0.00 ± 0.03	6.0/99% → 3.3/89%	multiple passes
Bottom $\phi = 0$ direct→10 °azimuthal	O 140 GHz	$0.35 \pm 0.25 \rightarrow$ 0.67 ± 0.12	2.8/98% → 3.7/100%	multiple peaks
Inboard-lower $\phi = 0$ direct→25 °attitudinal→ 25 °attitudinal & 15 °azimuthal	O 115 GHz	$0.35 \pm 0.04 \rightarrow$ $0.00 \pm 0.03 \rightarrow$ 0.22 ± 0.03	10/98% → 5.5/98% → 9.0/89%	multiple passes/peaks

In table 1 and figure 8 the explored options for ECRH can be seen. For this simple example only $\phi = 0$ (the bending point) is considered, later other spots along the reactor will be considered. Of note are:

- Outboard X-mode 140 GHz which has a great range and can very concentrated in the center. However if the density would increase significantly it might be cutoff.
- Outboard-upper O-mode 140 GHz mode also can heat the center surprisingly well but has a lesser range. It however would still be usable in case of a density increase.
- Inboard-lower O-mode 115 GHz is similar and can also heat the center pretty good but doesn't have a large range. But it also has a surprisingly low frequency.
- Inboard (slow-)X-mode can work but is not very concentrated and it not that well absorbed. This is likely caused by the relatively low temperature (see chapter 4.2.2). It however does use a very low frequency.

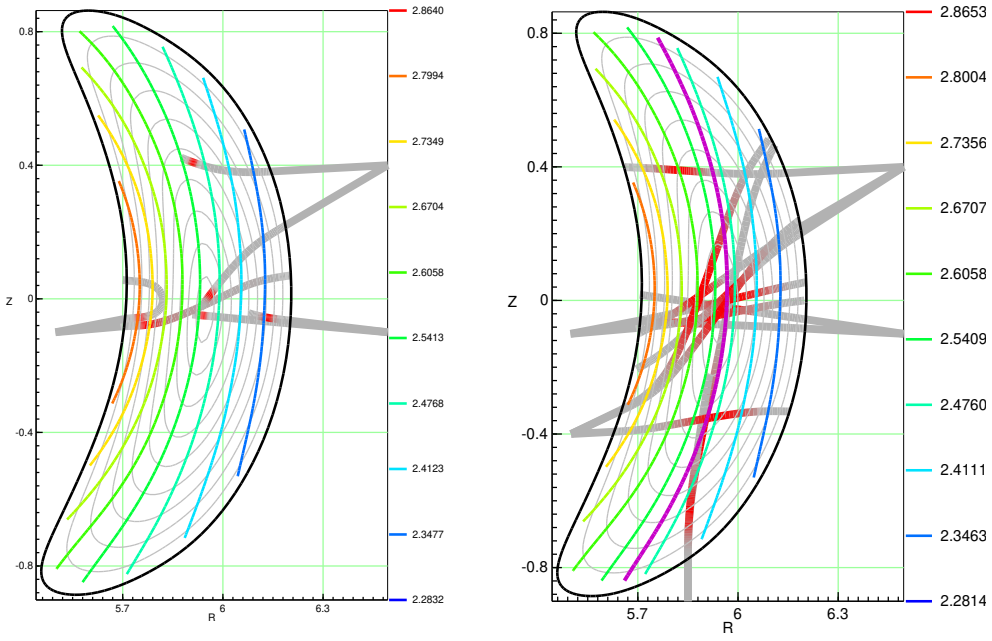

(a) The path and absorption of the X-mode beams.

(b) The path and absorption of the O-mode beams.

Figure 8: Paths of the beams from table 1. To ensure readability only a single pass of each beam is shown. The colored contour lines indicate magnetic field strength (in Tesla).

3.2 ITER

While not a Stellarator ITER is a interesting upcoming fusion reactor which will also need heating via ECRH. The ITER parameters are $B_0 = 5.3$ T, $n_{e0} = 1 \cdot 10^{20}$ /m^3 and $T_{e0} = 25$ KeV with $R = 6.2$m and $a = 2$ m [2].

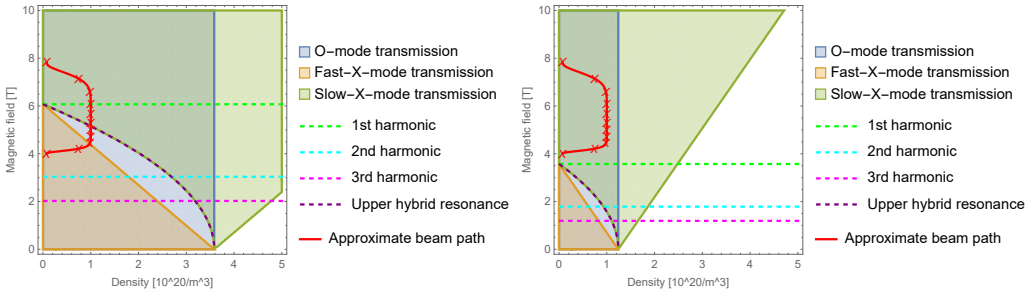

(a) 170 GHz beam.

(b) 100 GHz beam.

Figure 9: Regions of transmission and resonance in ITER ($B_0 = 5.3$ T, $n_{e0} = 1 \cdot 10^{20}$/m^3).

The density of ITER is not that high while at the same time the magnetic field is relatively high. Thus the first harmonic of 148 GHz is accessible using O-mode and slow-X-mode (see figure 9). In fact transmission of O-mode is possible down to 90 GHz. However due to the high magnetic field it is not feasible to use fast-X-mode since that would need to have a frequency around the second harmonic which is too high. Also as can also be seen in figure 9 and 10 the low aspect ratio causes a very large difference in magnetic strength from the low-field to the high-field side, this could be a useful property to exploit for ECRH.

In reality ITER will use two beams from the outboard and the outboard-upper side both at 170 GHz. The outboard beam will have a azimuthal range from 20° to 45° and the outboard-upper

beam will be azimuthally positioned at 20° with a attitudinal range of ±8° [10]. These beams can be seen in table 2 and figure 10a and their ECRH range approximately matches the real design specifications (outboard 0 → 0.6 r/a, outboard-upper 0.7 → 0.83[10]) with the any difference likely being explained by the fact that the positioning likely was not perfectly reproduced in Travis. Their power depositions are also incredibly concentrated (with the outboard aimed at achieving up to 56 MW/m).

Table 2: Several beam possibilities for an reactor like ITER. The absorption location is the peak absorption per volume as a fraction of the minor radius and the variation is given in half-width-half-maximum (HWHM). The height of the peak (in case of a 1 MW beam) also is given and can also be seen as a indication of concentration.

Beam location and direction	**Mode and frequency**	**Absorption peak (r/a)**	**Peak (MW/m)/ Absorption**	**Note**
Outboard 23° azimuthal→45 °azimuthal	O 170 GHz	$0.57 \pm 0.07 \rightarrow$ 0.00 ± 0.02	6.7/100% → 56/100%	planned ITER beam
Outboard-upper 8° attitudinal→ −8° attitudinal	O 170 GHz	$0.85 \pm 0.03 \rightarrow$ 0.75 ± 0.02	41/99% → 49/100%	planned ITER beam
Outboard direct→25 °azimuthal	O 147 GHz	$0.00 \pm 0.02 \rightarrow$ 0.43 ± 0.05	30/100% → 22/99%	multiple passes
Outboard-upper 5 °attitudinal→-65 °attitudinal→ -65 °attitudinal & 20 °azimuthal	O 147 GHz	$0.88 \pm 0.01 \rightarrow$ $0.12 \pm 0.03 \rightarrow$ 0.10 ± 0.01	48/100% → 16/100% → 36/100%	
Inboard direct→25 °azimuthal	X 100 GHz	$0.03 \pm 0.01 \rightarrow$ 0.28 ± 0.08	14/100% → 5/100%	
Inboard direct→25 °azimuthal	O 100 GHz	$0.09 \pm 0.02 \rightarrow$ 0.23 ± 0.03	18/100% → 11/100%	
Inboard-lower 20 °attitudinal→53 °attitudinal→ 53 °attitudinal & 20 °azimuthal	X 98 GHz	$0.63 \pm 0.02 \rightarrow$ $0.00 \pm 0.01 \rightarrow$ 0.03 ± 0.02	17/98% → 10/100% → 9/99%	

The options which were explored for this report can also be found in table 2 and figure 10b. Of particular note are:

- Outboard 147 GHz O-mode is an interesting alternative to the real life beams. It has less range (and flexibility) but it does use a lower frequency. Similarly the outboard-upper 147 GHz O-mode also is lower frequency but it does has a significantly better range than the real life counter-part. However this is likely caused by a larger range of aiming angles (16° total versus 70°).
- Inboard 100 GHz (slow-)X-mode works quite good, the power concentration is acceptable but most interestingly the frequency is very low. Surprisingly O-mode also works in the same configuration. However such a configuration would of course be hard to implement in reality due to the central solenoid taking up most of the inboard space.
- Inboard-lower 98 GHx (slow-)X-mode is the most interesting option of all. It a good range (same as outboard 170 GHz O-mode) with decent concentration, again a very low frequency and most importantly it is positioned near a spot where ECRH insertion might be feasible for a Tokamak [9].

So contrary to W7X here, due to the higher strength and gradient in the magnetic field slow-X-mode can work well.

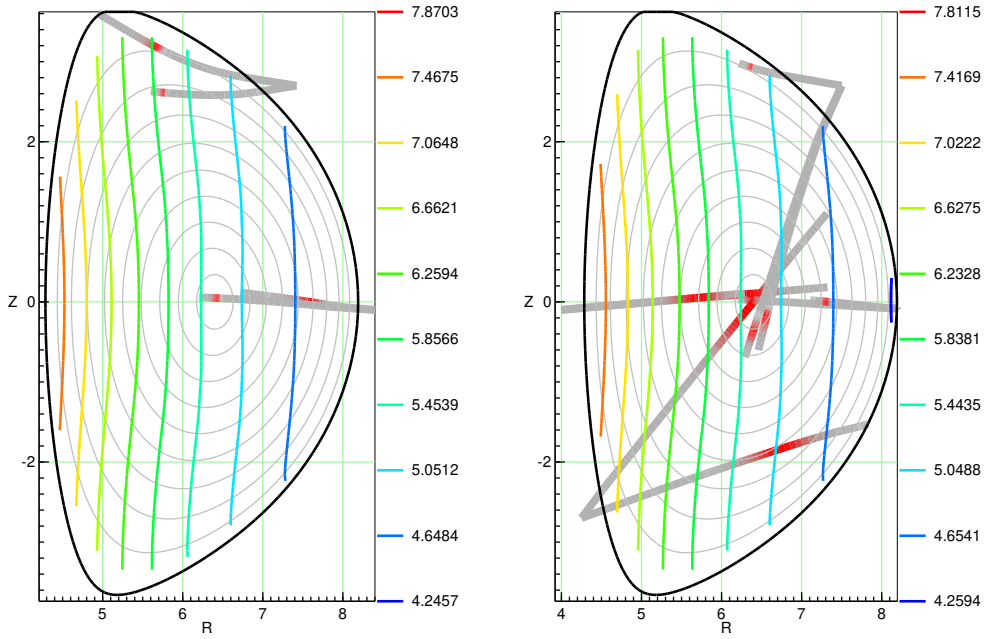

(a) The planned ERCH beams in the real ITER.

(b) Hypothetical beams.

Figure 10: Paths of the beams from table 2. The colored contour lines indicate magnetic field strength (in Tesla).

3.3 Wendelstein 7X high density

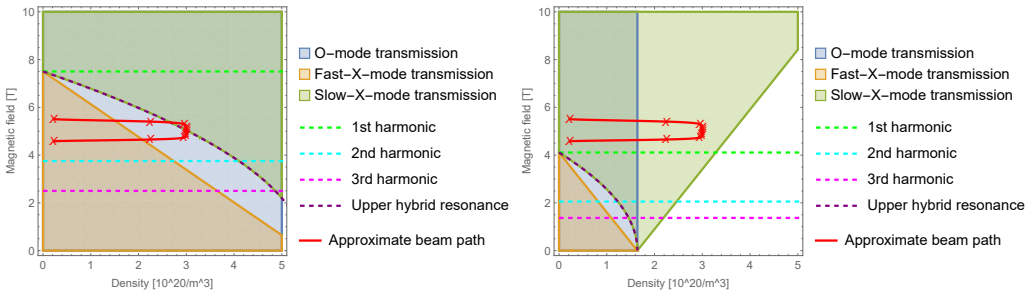

(a) 210 GHz beam.

(b) 115 GHz beam.

Figure 11: Regions of transmission and resonance in a hypothetical high-field Wendelstein 7X ($B_0 = 5$ T, $n_{e0} = 3 \cdot 10^{20}/\mathrm{m}^3$).

Another interesting case would be a hypothetical version of Wendelstein 7X which runs at a much higher magnetic field $B_0 = 5$ T, higher density $n_{e0} = 3 \cdot 10^{20}$ /m^3 (with a flat profile) and higher temperature $T_{e0} = 20$ KeV. The magnetic configuration and vessel say the same. This is a nice initial approximation of a potential future Stellarator.

Along the entire reactor the strength and range of the magnetic field stays approximately the same (see figure 12). For such a configuration the core it cutoff at approximately 155 Ghz for O-mode, 240 Ghz for (fast-)X-mode and 100 GHz for slow-X-mode with the first harmonic in being at 140 GHz. Thus only slow-X-mode and a (relativly) high frequency O-mode are possible. Contrary to chapter 3.1, where the real Wendelstein 7X was investigated, here several positions along the length of the reactor will be considered.

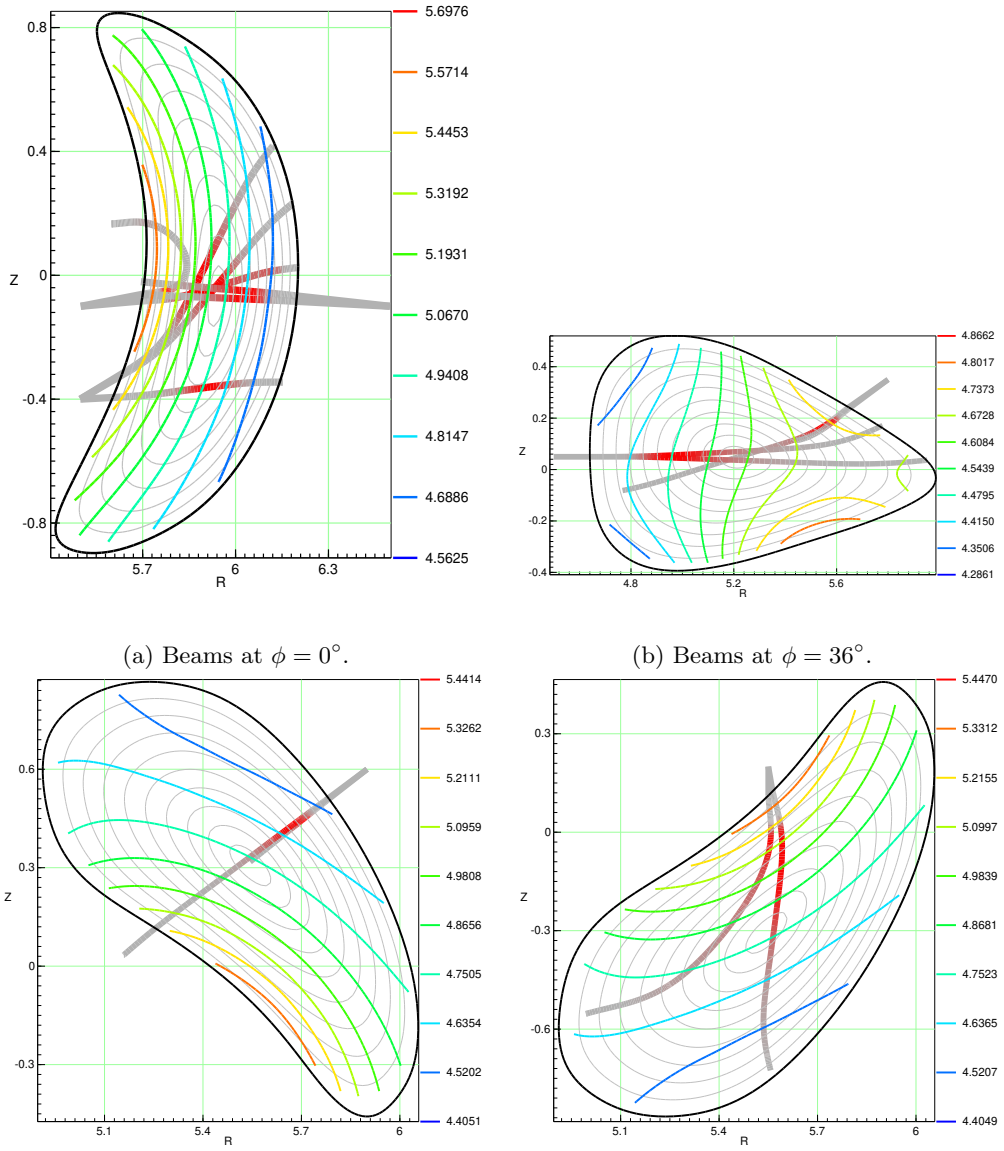

(a) Beams at $\phi = 0°$.

(b) Beams at $\phi = 36°$.

(c) Beams at $\phi = 18°$.

(d) Beams at $\phi = 54°$.

Figure 12: Paths of the beams from table 3. To ensure readability only a single pass of each beam is shown. The colored contour lines indicate magnetic field strength (in Tesla).

First of all at $\phi = 0°$ (the bending point of the Stellarator, see figure 12a) the magnetic profile is very similar to before, with the high-field on the inboard side and the low-field on the outboard side. Thus similar solutions to before can used: O-mode from both outboard(-upper) and inboard(-lower) and slow-X-mod from the inboard(-lower) side.

Moving to $\phi = 18°$ ($\frac{1}{4}$ of the periodicity, see figure 12c) the magnetic profile still is relatively simple but it has the high-field at the bottom and low-field at the top. From the high-field side there is potential for a slow-X-mode beam. A higher frequency O-mode could also work from both sides. It should be noted that the $\phi = 54°$ ($\frac{3}{4}$ of the periodicity, see figure 12d) is mirror symmetric with $\phi = 18°$.

Finally at $\phi = 36°$ ($\frac{2}{4}$ of the periodicity, see figure 12b) the magnetic profile has an interesting egg shape. The inboard-side is the low-field, outboard-upper and outboard-lower are the high-field while outboard is very similar to the center. This configuration also has a slightly lower magnetic field strength (around 4.5 Tesla). Interestingly slow-X-mode could be attempted

from the outboard-upper/lower while from the inboard side O-mode could be tried at a still high frequency but lower than other locations along the reactor.

Table 3: Several beam possibilities for an high density reactor like W7X. The absorption location is the peak absorption per volume as a fraction of the minor radius and the variation is given in half-width-half-maximum (HWHM). The height of the peak (in case of a 1 MW beam) also is given and can also be seen as a indication of concentration.

Beam location and direction	**Mode and frequency**	**Absorption peak (r/a)**	**Peak (MW/m)/ Absorption**	**Note**
Outboard $\phi = 0°$ direct→20 °azimuthal	O 210 GHz	$0.07 \pm 0.04 \rightarrow$ 0.10 ± 0.04	$2.6/80\% \rightarrow$ $0.6/16\%$	multiple passes/peaks
Inboard $\phi = 0°$ direct→25 °azimuthal	X 115 GHz	$0.05 \pm 0.02 \rightarrow$ 0.67 ± 0.10	$2.8/94\% \rightarrow$ $4.4/97\%$	wide tails of distribution
Inboard $\phi = 0°$ direct→25 °azimuthal	O 225 GHz	$0.04 \pm 0.02 \rightarrow$ 0.00 ± 0.01	$5.7/99\% \rightarrow$ $4/89\%$	multiple passes
Inboard-lower $\phi = 0°$ direct→30 °attitudinal→ 30 °attitudinal & 20 °azimuthal	O 225 GHz	$0.36 \pm 0.04 \rightarrow$ $0.02 \pm 0.02 \rightarrow$ 0.20 ± 0.03	$14/100\% \rightarrow$ $7.5/100\% \rightarrow$ $10/99\%$	
Outboard-upper $\phi = 18°$ direct→20 °azimuthal	O 225 GHz	$0.67 \pm 0.10 \rightarrow$ 0.00 ± 0.02	$4.6/100\% \rightarrow$ $0.9/95\%$	similar possible at outboard-lower $\phi = 54°$
Outboard-upper $\phi = 36°$ direct→20 °azimuthal	X 115 GHz	$0.12 \pm 0.03 \rightarrow$ 0.83 ± 0.11	$1.1/100\% \rightarrow$ $9/100\%$	wide tails of distribution
Inboard $\phi = 36°$ direct→20 °azimuthal	O 200 GHz	$0.03 \pm 0.02 \rightarrow$ 0.14 ± 0.04	$2.4/92\% \rightarrow$ $4.8/87\%$	wide tails of distribution
Inboard-upper $\phi = 54°$ direct→10 °attitudinal	X 115 GHz	$0.00 \pm 0.04 \rightarrow$ 0.29 ± 0.03	$2.7/100\% \rightarrow$ $8.2/100\%$	similar possible at inboard-lower $\phi = 18°$

All the explored options can be found in table 3 and figure 12 but the most interesting are:

- Inboard $\phi = 0°$ 115 GHz (slow-)X-mode which has a very decent range, an acceptable concentration and a very reasonable frequency.
- Inboard-lower $\phi = 0°$ 225 GHz O-mode is able to concentrate very well at the center. It however has frequency which is quite high and very little range.
- Inboard $\phi = 36°$ 200 GHz O-mode is a very interesting option. The center is heated pretty well but it is not the most concentrated but due to the lower field strength at this part of the reactor it is able to lower the frequency significantly compared to other O-mode options.
- Inboard-upper $\phi = 54°$ 115 GHz (slow-)X-mode again works acceptably for the center, although the power concentration could be better.

From these results it also appears that for such a hypothetical high-field Wendelstein 7X heating is best done from the inboard side. Because while there are options from the outboard-side they are often not that good.

3.4 SQuID reactor

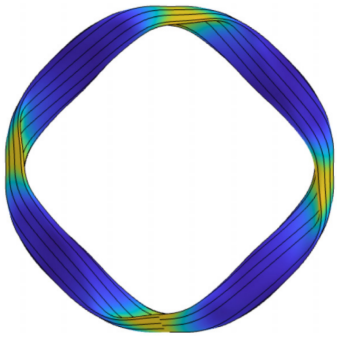

Figure 13: The SQuID magnetic configuration. Image taken from [5].

There is no concrete design for a future Stellarator reactor yet however recently a new magnetic configuration called SQuID was developed by a team led by Allan Goodman from the Max Planck Institute for Plasma Physics in Greifswald [5]. This optimized magnetic configurations has a shape that could be described as a rounded square (see figure 13) and thus has a periodicity of 90°. A magnetic strength is taken as $B_0 = 5.7$ T [5] however as discussed later the magnetic profile and strength varies greatly along the reactor. The major radius is approximately $R \approx 17$ m and the minor radius is $a \approx 2.5$ m. The conditions in the reactor have been set to $n_{e0} = 3 \cdot 10^{20}$ /m^3 (with a flat profile) and $T_{e0} = 20$ KeV.

As can be seen in figure 15 the magnetic profiles along the reactor are a lot more varied an unique than previously. These differences might offer opportunities to design ECRH beams. These will be investigated.

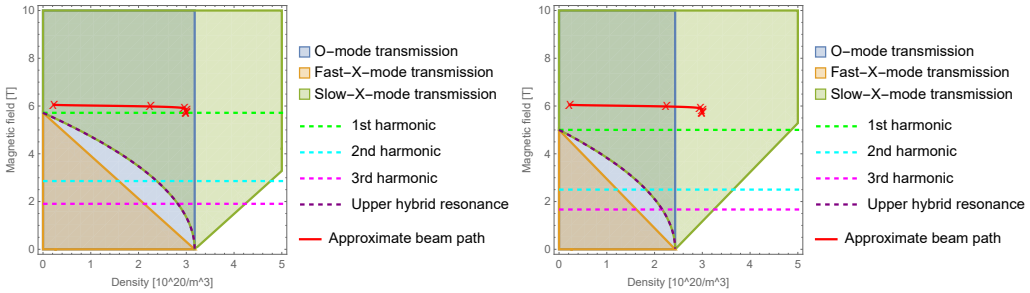

(a) 160 GHz beam, side to side at $\phi = 0°$.

(b) 140 GHz beam, side to side at $\phi = 0°$.

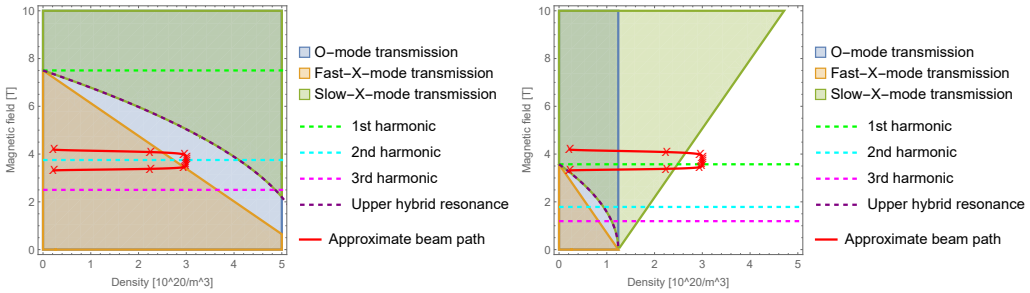

(c) 210 GHz beam, high to low-field at $\phi 22.5°$ and $\phi = 67.5°$.

(d) 100 GHz beam, high to low-field at $\phi 22.5°$ and $\phi = 67.5°$.

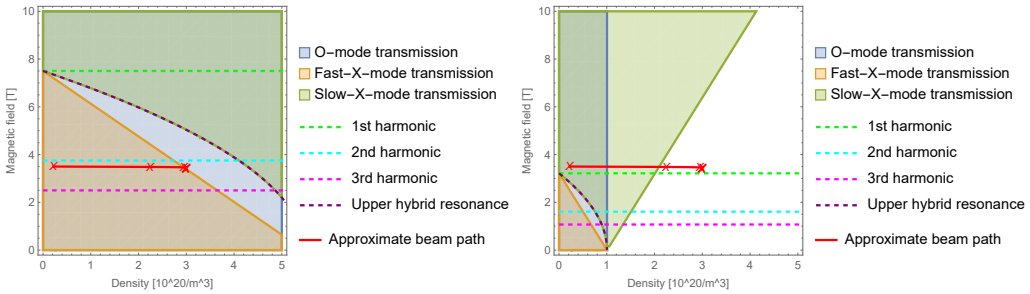

(e) 210 GHz beam, top to bottom at $\phi = 45°$.

(f) 90 GHz beam, top to bottom at $\phi = 45°$.

Figure 14: Regions of transmission and resonance in the SQuID configuration at various places along the reactor ($B_0 = 5.7$ T, $n_{e0} = 3 \cdot 10^{20}/\mathrm{m}^3$).

At $\phi = 0°$ (the bending point) there is a very interesting magnetic profile (see figure 15a). A saddle-point can be seen where at the top and bottom the magnetic field is weaker then the center but at the sides the magnetic field is higher than the center. The total gradient is not that high (only around 0.3 T) but this saddle-point, which is somewhat point-symmetric, could be very suitable to exploit, especially for slow-X-mode (see figure 14b). O-mode is possible in theory but likely not in practice since the cutoff conditions are almost matched in the center (see figure 14a). The plasma also is very elongated which can be used to heat the edge.

Next at $\phi = 22.5°$ ($\frac{1}{4}$ of the periodicity, see figure 15c) which is mirror-symmetric with $\phi = 67.5°$ ($\frac{3}{4}$ of the periodicity, see figure 15d) a more conventional magnetic profile can be seen with the low-field and high-field being at the top and bottom. The magnetic field also is significantly weaker at around 3.6 T in the center, however most of the gradient is concentrated in a corner near the high-field side. There is potential for a O-mode but it might not be trivial (see figure 14c). Slow-X-mode surprisingly is not possible because the magnetic field is to low which causes the first harmonic to be in cutoff (see figure 14d).

Finally at $\phi = 45°$ ($\frac{2}{4}$ of the periodicity, see figure 15b) again a egg-like shape can be seen. But this time the magnetic profile is very much like a valley with the high-field on top and bottom. The magnetic field also is relatively weak at only 3.4 T in the center. But the gradient also is very small with the field only being 0.1 T higher near the top/bottom. O-mode and perhaps

even fast-X-mode may be possible at the second harmonic due to this low magnetic field (see figure 14e), however the results might not be good due to the very low gradient in magnetic field. Again due to the low magnetic field slow-X-mode is not possible (see figure 14f)

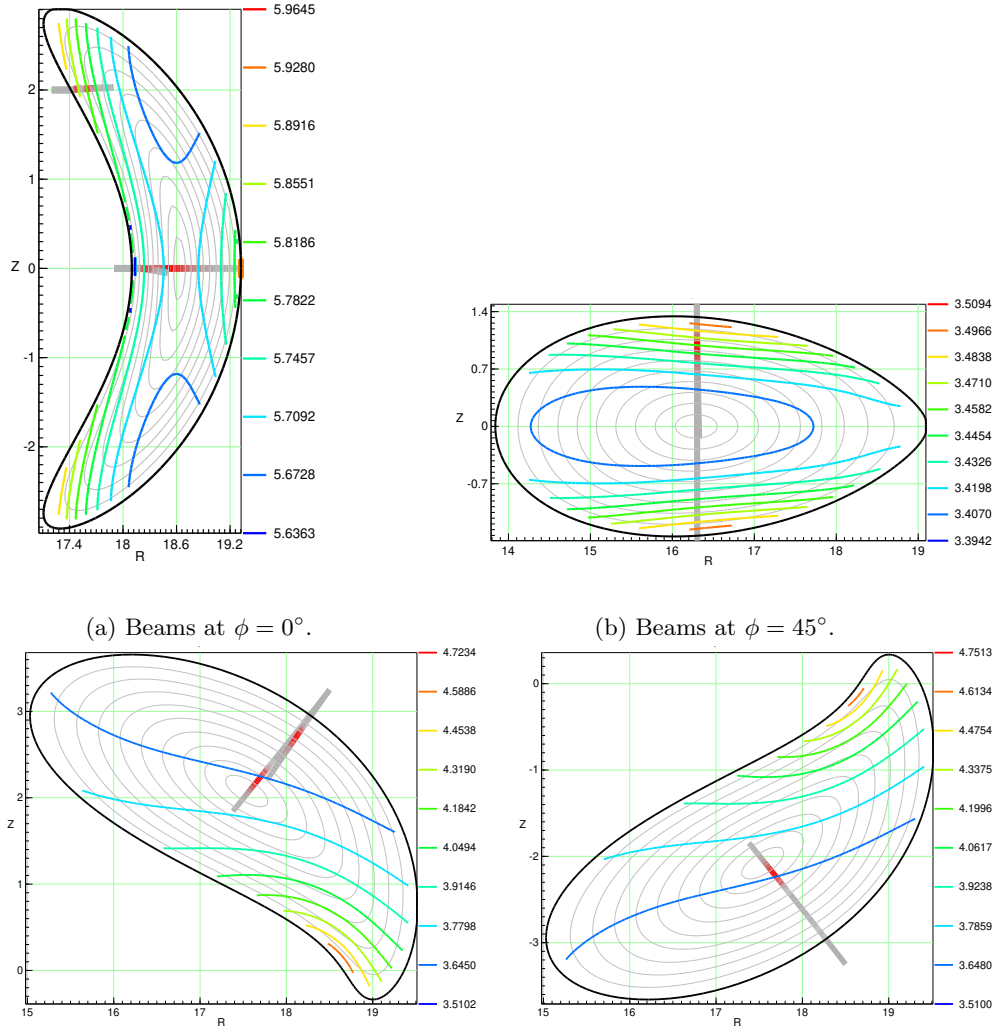

(a) Beams at $\phi = 0°$.

(b) Beams at $\phi = 45°$.

(c) Beams at $\phi = 22.5°$.

(d) $\phi = 67.5°$ with mirrored beams of $\phi = 22.5°$.

Figure 15: Paths of the beams from table 4. To ensure readability only a single pass of each beam is shown. The colored contour lines indicate magnetic field strength (in Tesla).

In figure 15 and table 4 an overview of the interesting beam options can be found. They are all interesting:

- Inboard $\phi = 0°$ 125 GHz slow-X-mode is an great option. It heats the center very well, has a great range and a very low frequency. Additionally it is also possible to have this beam from the outboard-side due to the symmetry of the saddle-point. Furthermore if a different frequency is used this beam can also be used to target more towards the edge of the plasma.
- Inboard-upper $\phi = 0°$ 150 GHz slow-X-mode works great for heating the edge is desired. The precise range can be adjusted by changing the frequency of the gyrotrons depending on what exactly are the design requirements.
- Outboard-upper $\phi = 22.5°$ 210 GHz O-mode is another great result. It can concentrate heat in the center and has a very large range. It also is possible further along the reactor at $\phi = 67.5°$.

- Top $\phi = 45°$ 210 GHz O-mode doesn't manage to concentrate its heating in the center and that shows that gradient of the magnetic profile is not large enough at that point in the reactor.

From this it can be seen that the magnetic profiles of SQuID are very unique and can be exploited. Furthermore there are quite a few good options for SQuID which is great for flexibility in case such a reactor every gets build.

Table 4: Several beam possibilities for the SQuID reactor. The absorption location is the peak absorption per volume as a fraction of the minor radius and the variation is given in half-width-half-maximum (HWHM). The height of the peak (in case of a 1 MW beam) also is given and can also be seen as a indication of concentration.

Beam location and direction	**Mode and frequency**	**Absorption peak (r/a)**	**Peak (MW/m)/ Absorption**	**Note**
Inboard $\phi = 0°$ direct→25 °azimuthal	X 125 GHz	$0.00 \pm 0.01 \rightarrow 0.65 \pm 0.10$	4.2/99% → 5.4/100%	similar possible from outboard
Inboard $\phi = 0$ direct→25 °azimuthal	X 140 GHz	$0.37 \pm 0.25 \rightarrow 0.83 \pm 0.05$	3.0/100% → 8.7/100%	similar possible from outboard
Inboard-upper $\phi = 0°$ direct→25 °azimuthal	X 150 GHz	$0.81 \pm 0.06 \rightarrow 0.93 \pm 0.03$	12/100% → 25/100%	similar possible from inboard-lower
Outboard-upper $\phi = 22.5°$ direct→25 °azimuthal	O 210 GHz	$0.00 \pm 0.02 \rightarrow 0.77 \pm 0.08$	5.5/100% → 5.0/100%	similar possible at outboard-lower $\phi = 67.5°$
Top $\phi = 45°$ direct→10 °azimuthal	O 210 GHz	$0.00 \pm 0.03 \rightarrow 0.72 \pm 0.12$	0.5/98% → 4.0/100%	wide tails of distribution

4 Conclusion

4.1 Conclusion

In this report different ECRH techniques were investigated. This was done through a region-plot which clearly shows regions of transmission and cutoff in which a parametric plot of the beam can be made to quickly/easily estimate if an ECRH beam is possible. To more accuratly simulate ECRH beams a ray tracing code, Travis, was used. To use this software many compatibility problems had to be solved and some extra tools were developed.

These techniques were implemented to (re)design ECRH beams for Wendelstein 7X, ITER, a hypothetical high-field Wendelstein 7X and the SQuID magnetic configurations, which represent a potential future Stellarator reactor. For each device a few good options were found. For Tokamaks/ITER slow-X-mode from the inboard-lower side showed great results in having concentrated heating with relatively low frequencies. For Stellarators the magnetic profile along the device needed to be investigated and in general slow-X from the high-field side, if the magnetic field was high enough, and higher frequency O-mode, if the density and/or the magnetic field was not to high, had good results.

Of specific interest was the SQuID configuration for which it was found that the saddle-point near the bending points could be exploited for slow-X-mode from both inboard, outboard, outboard-upper and outboard-lower to cover the entire range of the reactor. A bit further along the reactor a more conventional profile can be found which happens to have a significantly lower magnetic field which enables effective use of O-mode.

4.2 Discussion

Two mistakes were made, the power concentration/depositions was evaluated in power per volume and the effects of temperature were not taken into account (this will be discussed later), but in general the author is satisfied with the obtained results. However as the title suggests these are the "first steps" and more research should be done. Of particular interest would be further development and research of slow-X-mode ECRH.

Furthermore more research into SQuID and how to exploit its unique magnetic profile would be interesting. Perhaps instead of only looking at 4 evenly divided sections per periodicity a more gradual investigation could be done. The effect of azimuthal injection angles, which cause a beam to travel along the reactor through the different sections, is also interesting and could result in useful magnetic gradients along the beam path. It would also be interesting to investigate other magnetic configurations that could be used for future reactors.

Finally Bernstein waves also were not accomplished/used in this report. It should be further investigated how such waves could be used and how best to design them.

4.2.1 Power concentration

During the presentation of the results a criticism given was that using power absorption per volume may be biased due to the singularity at $r = 0$. The authors initial logic was that heat capacity is depended on volume and thus power per volume is proportional to temperature increase/heating. However this could cause a situation where the majority of the heat is absorbed at the edge but the tiny amount of heat that reaches the center still causes a peak to be visible there. Thus a better measure might be the absorbed power per radius/distance. These values were hastily added after the presentation and used in comparisons of beams. However this is a imperfect method and for future research this or a comparable measure should be the focus when evaluating/designing ECRH beams.

4.2.2 Temperature dependence

Finally it was also pointed out that (slow-)X-mode absorption also is heavily depended on temperature and that the temperature of $T_{e0} = 20$ KeV was quite high for a reactor at a density

of $n_{e0} = 3 \cdot 10^{20}$ /m^3. These effects had indeed not been taken into account, so a quick investigation was done.

In figure 16 the effect of the temperature can be seen on the inboard and inboard-upper slow-X-mode beams (and their different angles) of the SQuID configuration. Indeed as the temperature decreased the absorption decreased. While not directly visible the reduced absorption due to the temperature thus 'pushes' the peak further into the plasma. Thus (as can also be seen) adjusting the angle to be larger can mitigate the effects of the lower temperature. Furthermore higher frequencies also counteract this effect (as can be seen from the inboard-upper beam which has a higher frequency). Thus any effects that the misjudged temperature had can likely by accounted for in the design.

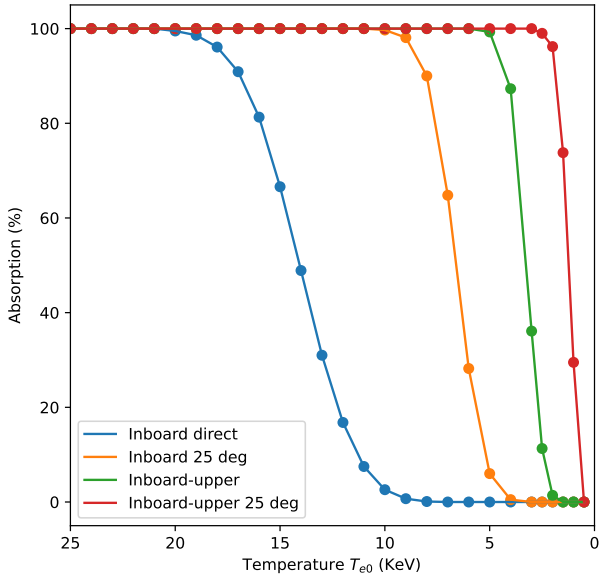

Figure 16: Absorption of beams from the SQuID design versus (core) temperature. Specifically inboard $\phi = 0°$ 125 GHz slow-X-mode and inboard-upper 150 GHz slow-X-mode (see table 4).

However regardless of the size of the effect and potential ways to reduce the effect the temperature and its effect should be taken into better account and studied further.

4.3 Acknowledgments

I would like to thank Neha Chaudhary for being my project supervisor, she provided me with great guidance and lots of good ideas and Felix Warmer for being my academic supervisor. I would also like to thank the Technical University of Eindhoven for paying for my housing in Greifswald and the Max Planck Institute for Plasma Physics for offering the internship. Furthermore I am grateful for the help provided by Alan Goodman, Joachiem Geiger and Timo Bogaarts who respectfully provided the SQuID file, help converting the file and the Python package to convert it to a vessel file. Finally I would like to thank my fellow intern Ivo Heldt who, besides being a good rubber-duck, I had lots of fun talking and sometimes playing a quick boardgame with.

References

[1] Pavel Aleynikov and Nikolai Marushchenko. ECRH and mode conversion in overdense W7-X plasmas. In *27th IAEA Fusion Energy Conference, Gandhinagar*, 2018.

[2] R Aymar, P Barabaschi, and Y Shimomura. The ITER design. *Plasma physics and controlled fusion*, 44(5):519, 2002.

[3] Johan Buermans, K. Crombé, L. Dittrich, A. Goriaev, Yu. Kovtun, S. Möller, D. López-Rodríguez, P. Petersson, M. Verstraeten, and T. Wauters. X-mode electron cyclotron heating scenarios beyond the cut-off density. *AIP Conference Proceedings*, 2984(1):110003, 08 2023.

[4] N.L. Cardozo. Fusion on the back of an envelope (3MF100), 2022.

[5] Alan G Goodman, Pavlos Xanthopoulos, Gabriel G Plunk, Håkan Smith, Carolin Nührenberg, Craig D Beidler, Sophia A Henneberg, Gareth Roberg-Clark, Michael Drevlak, and Per Helander. Quasi-isodynamic stellarators with low turbulence as fusion reactor candidates. *PRX Energy*, 3(2):023010, 2024.

[6] Hans-Jurgen Hartfuss and Thomas Geist. *Fusion plasma diagnostics with MM-waves an introduction*. Wiley-VCH, 2013.

[7] Qiao Liu, Xinjian Niu, Yinghui Liu, Jianwei Liu, Lina Wang, and Jie Qing. Investigation on a 170 GHz/230 GHz Dual Mode Megawatt-class Gyrotron For CFETR. In *2020 IEEE 21st International Conference on Vacuum Electronics (IVEC)*, pages 263–264. IEEE, 2020.

[8] Nikolai B Marushchenko, Yu Turkin, and Henning Maaßberg. Ray-tracing code TRAVIS for ECR heating, EC current drive and ECE diagnostic. *Computer Physics Communications*, 185(1):165–176, 2014.

[9] Vladimir F Shevchenko, Erasmus Du Toit, Andrei Fokin, Evgeniy Tai, Tim Bigelow, and John B Caughman. 2 MW ECRH system for ST40 spherical Tokamak. In *2021 46th International Conference on Infrared, Millimeter and Terahertz Waves (IRMMW-THz)*, pages 1–2. IEEE, 2021.

[10] H Zohm. The concept of ECRH/ECCD for ITER. In *13th Joint Workshop on Electron Cyclotron Emission and Electron Cyclotron Resonance Heating (EC-13)*, 2004.

A Travis tutorial

Travis is a powerful ray tracing code which can be used to do ECE calculations or, relevant for this, report ECRH calculations [8]. This section serves as a small tutorial for anyone who might be interested. Furthermore it also documents some of the tools which were developed during the internship.

The tools which were developed can be found on this Github `https://github.com/TimHeiszwolf/IPP_ECRH_internship`. Note that some software/files/etc (such as Travis itself or SQuID) are not on there since the author of this report doesn't have permission to share those. So if those are desired please contact the relevant people at IPP.

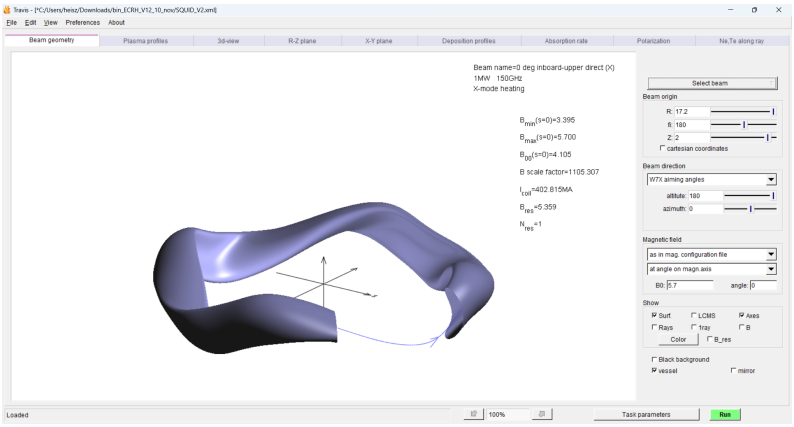

Figure 17: A screenshot of the Travis GUI with the SQuID configuration loaded.

The easiest way to use Travis is with the GUI (see figure 17). It can also be used as part of a Java/Matlab/etc script, which can be useful for doing large/automated tasks like a parameter sweep. To do a simulation Travis requires a few things:

- A magnetic configuration. Note that this doesn't specify the absolute magnetic field strength (that is done in the project file).
- A vessel file which specifies the vessel and is calculated from the magnetic configuration.
- A mirror file (optional) which can either be made manually or generated with the vessel file.
- A project file, which refers to the above 3 files, contains the settings and most importantly also contains the beam descriptions and reactor/plasma conditions.

A.1 Magnetic configuration

The magnetic configuration file specifies what the magnetic profiles look like, it is the file from which all the other parts are (indirectly) based on. If a magnetic profile is needed it can be helpful to look at the VMEC database `http://svvmec1.ipp-hgw.mpg.de:8080/vmecrest/v1` (only accessible from IPP). The most commonly used file format is .nc (netCDF), which also is what is needed to make a vesselfile, however Travis doesn't accept this format. There are a few formats that are accepted but the easiest is the VMEC ascii/Wout.txt format. These often can be found on the VMEC database but conversion from the netCDF is possible. For this project Joachiem Geiger was kind enough to help with that since the author doesn't have much experience with VMEC.

A.2 Vessel file

The vessel file specifies the vessel by slicing the vessel into segments in ϕ (cross sections), each segment is then defined by the r and z points along the segment. Such a vessel file can be

generated using the SBGeom Python package from Timo Bogaarts `https://pypi.org/project/SBGeom/`. If you have trouble installing this package on Windows consider using Windows Subsystem for Linux by installing Ubuntu from the Microsoft store (since for Linux the package has been pre-compiled).

To make future work easier a script has been made which implements this SBGeom packaged. It can be found on the Git of this project (see start of chapter). It takes the magnetic configuration as input, together with some settings, and then outputs a vessel file.

A.3 Mirror file

The mirror file is a XML file containing all the polygons of the mirrors for your simulation. The polygons can be manually specified however that is a very time consuming tasks. Thus a script was made to easily make some mirrors (see git at the start of the chapter).

It simply takes the coordinates of the vessel file within a certain specified range, adds a margin and converts it into polygons. The user gives a range in ϕ and z (specifying inboard or outboard). It should be noted that since this is a script focused on easy of use there are some limitations. For example complex mirror shapes are not really possible (only rectangles), it is not possible to place mirrors at the top or bottom of the vessel (since it is based on a z range and not a θ range) and the direction of the mirror can't be specified (it will always be parallel to the wall).

A.4 Project file

Finally the project file is where all these things come together. It first contains some settings where the location the relevant files are specified. It also contains the reactor/plasma conditions (magnetic field strength, temperature, density, effective charge, etc). Finally it specifies the beams itself (starting location, direction, mode and frequency, etc).

Such a project file can be made/edited via text (good for editing many predictable things) or via the Travis GUI (useful for tweaking settings/beam positions). On the Git (see start of the chapter) a few examples can be found.